Adamantane-Based Wide-Bandgap Host Material: Blue Electrophosphorescence with High Efficiency and Very High Brightness

12 AUTHORS, INCLUDING:

Liping Zhu
Chinese Academy of Sciences
21 PUBLICATIONS   126 CITATIONS

SEE PROFILE

Jingui Qin
Wuhan University
480 PUBLICATIONS   10,777 CITATIONS

SEE PROFILE

Chuluo Yang
Wuhan University
174 PUBLICATIONS   4,846 CITATIONS

SEE PROFILE

■ Electrophosphorescence

Adamantane-Based Wide-Bandgap Host Material: Blue Electrophosphorescence with High Efficiency and Very High Brightness

Yu Gu,[a] Liping Zhu,[b] Yifan Li,[a] Ling Yu,[a] Kailong Wu,[a] Tianheng Chen,[a] Manli Huang,[a] Feng Wang,[a] Shaolong Gong,[a] Dongge Ma,*[b] Jingui Qin,[a] and Chuluo Yang*[a]

Abstract: An adamantane-based host material, namely, 4-{3-[4-(9H-carbazol-9-yl)phenyl]adamantan-1-yl}benzonitrile (CzCN-Ad), was prepared by linking an electron-donating carbazole unit and an electron-accepting benzonitrile moiety through an adamantane bridge. In this approach, two functional groups were attached to tetrahedral points of adamantane to construct an "sp³" topological configuration. This design strategy endows the host material with a high triplet energy of 3.03 eV due to the disruption of intramolecular charge transfer. Although CzCN-Ad has a low molecular weight, the rigid nonconjugated adamantane bridge results in a glass transition temperature of 89 °C.

These features make CzCN-Ad suitable for fabricating blue phosphorescent organic light-emitting diodes (PhOLEDs). The devices based on sky-blue phosphor bis[(4,6-difluorophenyl)pyridinato-N,$C^{2'}$](picolinato)iridium(III) (FIrpic) achieved a high maximum external quantum efficiency (EQE) of 24.1%, which is among the best results for blue PhOLEDs ever reported. Furthermore, blue PhOLEDs with bis(2,4-difluorophenylpyridinato)-tetrakis(1-pyrazolyl)borate iridium(III) (FIr6) as dopant exhibited a maximum EQE of 14.2% and a maximum luminance of 34262 cd m^{-2}. To the best of our knowledge, this is the highest luminance ever reported for FIr6-based PhOLEDs.

Introduction

Phosphorescent OLEDs (PhOLEDs) are currently attractive because of their theoretical 100% internal quantum efficiency due to effectively harvesting both singlet and triplet excitons.[1–3] Phosphorescent emitters typically have long exciton lifetimes and long diffusion lengths, which may lead to serious concentration quenching and T_1–T_1 annihilation at high current densities, and hence heavy-metal complexes of phosphors are usually doped into suitable host materials to suppress unfavorable behavior. In this regard, the development of suitable host materials is as important as developing efficient phosphors. For blue-emitting phosphors, a wide bandgap is the most demanding host-material criterion.[4–11] Some strategies for designing wide-bandgap host materials have been demonstrated. Thompson et al. initially reported a series of tetraaryl silicon compounds with ultrahigh triplet energies (≈ 3.5 eV) as host

materials.[12] We presented a series of silicon-bridged bipolar hosts with high triplet energies of up to 2.93 eV.[13] Fukagawa et al. constructed three adamantane-based host materials with triplet energies as high as 2.97 eV.[14–16] Kang et al. introduced a carborane cluster as bridge between N-phenylcarbazole units and obtained several host materials with high triplet energies around 3.05 eV.[17]

In this work, we designed and synthesized a new host material with adamantane as π-conjugation interrupter between N-phenylcarbazole and benzonitrile functional groups. We anticipated that the adamantane bridge would suppress intramolecular charge transfer from electron-donating carbazole to electron-accepting benzonitrile, and that this would endow the molecule with a high triplet energy. Besides, we hoped that the introduction of the rigid adamantane bridge would make the host thermally stable despite its low molecular weight, which would be beneficial to vacuum sublimation during device fabrication and device stability during operation. With the adamantane-based host material, a bis[(4,6-difluorophenyl)pyridinato-N,C2'](picolinato)iridium(III) (FIrpic)-based sky-blue device achieved a maximum external quantum efficiency (EQE) of 24.1%, and a bis(2,4-difluorophenylpyridinato)-tetrakis(1-pyrazolyl)borate iridium(III) (FIr6)-based blue device showed a maximum EQE of 14.2% and a maximum luminance of 34262 cd m^{-2}.

[a] Y. Gu, Y. Li, L. Yu, K. Wu, T. Chen, M. Huang, F. Wang, Dr. S. Gong, Prof. J. Qin, Prof. C. Yang
Hubei Collaborative Innovation Center for
Advanced Organic Chemical Materials
Hubei Key Lab on Organic and Polymeric Optoelectronic Materials
Department of Chemistry, Wuhan University, Wuhan 430072 (P. R. China)
E-mail: clyang@whu.edu.cn

[b] L. Zhu, Prof. D. Ma
State Key Laboratory of Polymer Physics and Chemistry
Changchun Institute of Applied Chemistry, Chinese Academy of Sciences
Changchun 130022 (P. R. China)
E-mail: mdg1014@ciac.jl.cn

Results and Discussion

Synthesis and characterization

The synthetic route to and chemical structure of the host material 4-{3-[4-(9H-carbazol-9-yl)phenyl]adamantan-1-yl}benzonitrile (CzCN-Ad) are depicted in Scheme 1. The important inter-
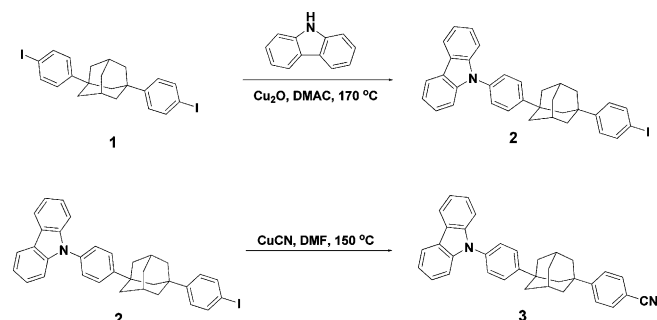
Scheme 1. Synthetic route to and chemical structure of CzCN-Ad.

mediate **2** was prepared in a moderate yield of 50% by the Ullmann C−N coupling reaction between the iodo-substituted adamantane precursor and carbazole in a precisely controlled ratio of 1:1. Then the remaining iodo group was replaced by a CN group to provide the desired product CzCN-Ad. The intermediate and final product were characterized by ^{1}H and ^{13}C NMR spectroscopy, mass spectrometry, and elemental analysis. Thermal, photophysical, and electrochemical data of CzCN-Ad are listed in Table 1. The thermal properties of CzCN-Ad were determined by thermogravimetric analysis (TGA) and differential scanning calorimetry (DSC), as shown in Figure 1. The decomposition temperature T_d corresponding to 5% weight loss of CzCN-Ad was 383°C. The compound showed a glass transition temperature T_g of 89°C despite its low molecular weight of only 478. For comparison, the widely used host CBP has the similar molecular weight of 484 but a low T_g of 62°C. Another Si-based bipolar host, namely, m-OXDSiTPA, has a higher molecular weight of 704 but a T_g of only 77°C.[18] The high T_g value of CzCN-Ad should be attributed to the introduction of the rigid adamantane unit.

Photophysical properties

Figure 2 shows the absorption, fluorescence, and phosphorescence spectra of CzCN-Ad. The absorption in the range of 310–350 nm and around 293 nm could be assigned to the π–π*
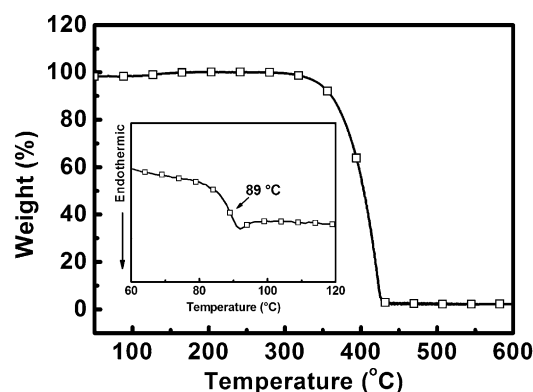

Figure 1. TGA trace of CzCN-Ad recorded at a heating rate of 10°C min^{-1}. Inset: DSC trace of CzCN-Ad recorded at a heating rate of 10°C min^{-1}.
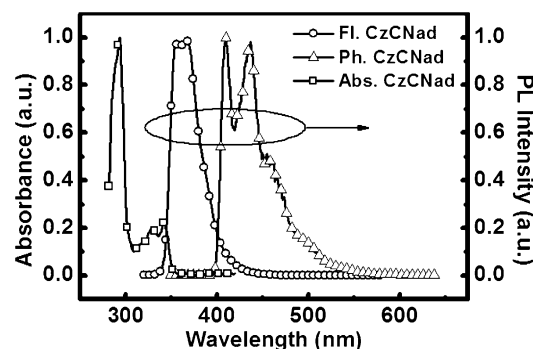

Figure 2. Normalized UV/Vis absorption and fluorescence spectra of CzCN-Ad in toluene at room temperature and phosphorescence spectrum of CzCN-Ad in 2-methyltetrahydrofuran at 77 K.

transition of the carbazole moiety.[19–21] The optical bandgap E_g estimated from the absorption edge is 3.52 eV. The compound shows two emission peaks at 356 and 366 nm. The triplet energy E_T of CzCN-Ad was determined to be 3.03 eV from the highest-energy vibronic subband in the phosphorescence spectrum. To evaluate the energy-transfer process between CzCN-Ad and the blue phosphors of FIrpic and FIr6, we measured the transient photoluminescence decay of 10 wt% FIrpic or FIr6 doped into CzCN-Ad. As shown in Figure 3, the CzCN-Ad:FIrpic and CzCN-Ad:FIr6 films exhibit single-exponential decay curves on the microsecond timescale of 1.52 and 3.25 μs, respectively. This can be attributed to the higher E_T of CzCN-Ad (3.03 eV) compared to FIrpic (2.65 eV) and FIr6 (2.72 eV) and is indicative of complete energy transfer from host to guest.[22] To further assess the superiority of CzCN-Ad as host material for blue guest FIr6, we measured the photoluminescence quantum yield (PLQY) of the film with 10 wt% FIr6 doped into CzCN-Ad. For comparison, we also measured the PLQY of the film with 10 wt% FIr6 dopant in TCTA. The CzCN-Ad:10 wt% FIr6 film exhib-

Table 1. Thermal, photophysical, and electrochemical data.

Compound	T_g[a] [°C]	T_d[b] [°C]	λ_{abs}[c] [nm]	$\lambda_{em,max}$[c] [nm]	HOMO[d]/LUMO[e] [eV]	E_g[f] [eV]	E_T[g] [eV]
CzCN-Ad	87	383	342, 293	366, 356	−5.62/−2.10	3.52	3.03

[a] Obtained by DSC. [b] Obtained by TGA. [c] Measured in toluene. [d] Determined from the onset of the oxidation potential. [e] Calculated from HOMO and E_g. [f] Bandgap was calculated from the absorption edge of the UV/Vis spectrum. [g] Measured in 2-methyltetrahydrofuran at 77 K.
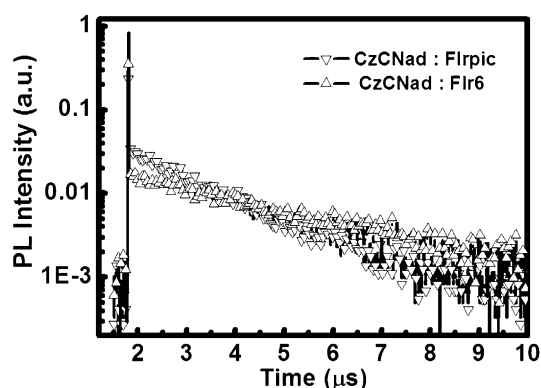
Figure 3. Decay of the PL intensity (excited at 330 nm) at room temperature for thin films of 10 wt % FIrpic or FIr6 doped into CzCN-Ad.

ited a higher PLQY of 72 % compared to TCTA:10 wt % FIr6 film (51 %), which suggests potential of CzCN-Ad as host for FIr6.

Electrochemical properties and DFT calculations

Cyclic voltammetry (CV) was performed to investigate the electrochemical properties of CzCN-Ad (Figure 4). The compound
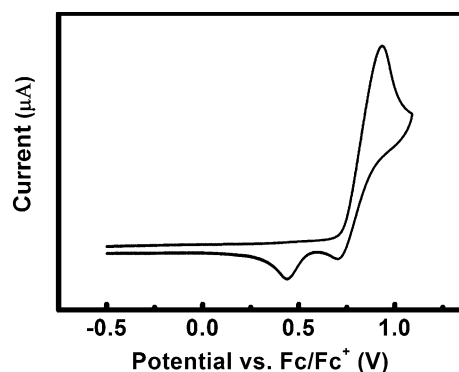

Figure 4. Cyclic voltammogram of CzCN-Ad in CH_2Cl_2 for oxidation.

exhibits irreversible oxidation waves like most carbazole derivatives, due to the instability of their radical cations.[23, 24] The HOMO energy level of CzCN-Ad was determined to be -5.62 eV from the onset of the oxidation potential with respect to the energy level of ferrocene (4.8 eV below vacuum), which is slightly lower than that of hole-transporting material TAPC (-5.5 eV).[25] The LUMO level deduced from E_g (3.52 eV) and the HOMO level is -2.10 eV, which is suitable for electron injection from the cathode.

DFT calculations [B3LYP, 6-31G(d)] were carried out to obtain a deeper understanding of the relationship between geometrical and electronic properties of the compound. According to the calculations, the HOMO is mainly localized on the electron-rich carbazole moiety, and the LUMO is distributed over the electron-deficient benzonitrile group (Figure 5). CzCN-Ad has almost complete separation of HOMO and LUMO at the electron-donor and electron-acceptor units due to the nonconjugated adamantane linkage.
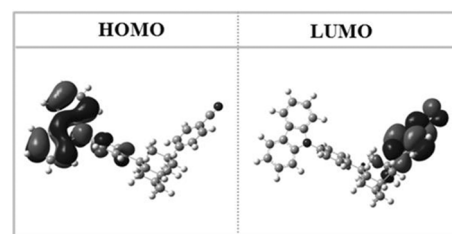

Figure 5. Calculated spatial distributions of the HOMO and LUMO of CzCN-Ad.

Device A

Device B

Device C

Device D

Figure 6. Configurations of devices A–D.

Electrophosphorescent devices

To evaluate CzCN-Ad as host for blue phosphorescent emitters, we initially designed the following FIrpic-based sky-blue device structure (device A, Figure 6; for definitions of abbreviations, see Experimental Section): ITO/MoO$_3$ (10 nm)/NPB (100 nm)/TCTA (5 nm)/CzCN-Ad:FIrpic (10 wt %, 20 nm)/TmPyPB (35 nm)/LiF (1 nm)/Al (100 nm), in which MoO$_3$ and LiF were used as hole- and electron-injecting layers, respectively, NPB and TmPyPB as the hole- and electron-transporting layers, respectively, TCTA was used as electron/exciton-blocking layer, and FIrpic doped into CzCN-Ad with optimized doping level of 10 wt % as emitting layer. TCTA and TmPyPB have higher triplet energies (TCTA, $E_T = 2.86$ eV; TmPyPB, $E_T = 2.78$ eV) than FIrpic to confine the exciton in the emitting layer. The current efficiency and power efficiency versus current density of the devices are shown in Figure 7, and the key device data are summarized in Table 2.

Remarkably, device A exhibited very high efficiency with a maximum current efficiency of 57.0 cd A^{-1}, a maximum power efficiency of 45.9 lm W^{-1}, and a maximum EQE of 24.1 % (Figure 8). These efficiencies are among the highest ever reported for FIrpic-based PhOLEDs.[26–39]
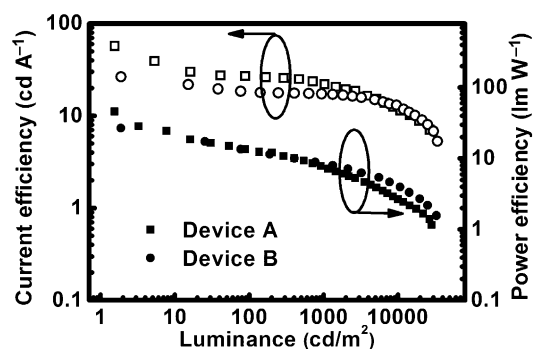
Figure 7. Current efficiency and power efficiency versus luminance curves for devices A and B.

Figure 9. Normalized EL spectra of device B at various voltages.

Table 2. Electroluminescence characteristics of devices A–D.

Device	L_{max}[a] [cd m^{-2}]	$\eta_{c,max}$[b] [cd A^{-1}]	$\eta_{p,max}$[c] [lm W^{-1}]	$\eta_{ext,max}$[d] [%]	CIE[e] (x, y)
A	28 547	57.0	45.9	24.1	0.17, 0.36
B	34 262	26.5	26.8	14.2	0.15, 0.25
C	21 715	26.2	22.5	14.1	0.15, 0.25
D	10 025	23.5	23.8	12.6	0.15, 0.25

[a] Maximum luminance. [b] Maximum current efficiency. [c] Maximum power efficiency. [d] Maximum EQE. [e] Commission International de l'Eclairage coordinates.
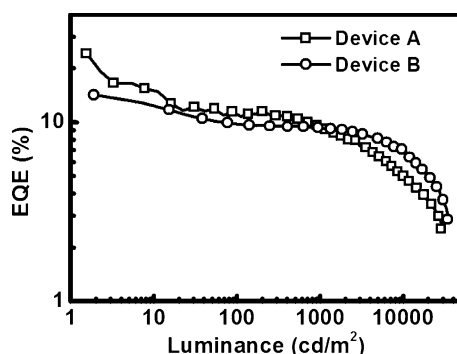

Figure 10. Current density–voltage–brightness characteristics of devices A and B.

Figure 8. EQE versus luminance curves for devices A and B.

Owing to the high E_T of 3.03 eV, CzCN-Ad could confine the excitons in the emitting layer, so we fabricated simplified device C [ITO/MoO$_3$ (10 nm)/TAPC (65 nm)/CzCN-Ad:FIr6 (10%, 20 nm)/TmPyPB (35 nm)/LiF (1 nm)/Al (100 nm)] without the TCTA exciton-blocking layer of device B. For comparison, device D with TCTA as host was also fabricated. The maximum external quantum efficiencies of devices C and D were 14.1 and 12.6% (Figure 11), respectively.

CzCN-Ad-hosted blue PhOLEDs showed better performance than TCTA-hosted devices under identical conditions. We presumed that CzCN-Ad could confine excitons in the emissive layer and suppress reverse energy transfer from the guest back to the host more efficiently than TCTA. To confirm this hypoth-

The E_T of CzCN-Ad (3.03 eV) is high enough to host blue phosphor FIr6 (2.72 eV), and we thus fabricated device B: ITO/MoO$_3$ (10 nm)/TAPC (60 nm)/TCTA (5 nm)/CzCN-Ad:FIr6 (10 wt%, 20 nm)/TmPyPB (35 nm)/LiF (1 nm)/Al (100 nm). Device B showed a maximum current efficiency of 26.5 cd A^{-1}, a maximum power efficiency of 26.8 lm W^{-1}, and a maximum EQE of 14.2%. The electroluminescence (EL) spectrum of device B showed typical and stable FIr6 emission with good CIE coordinates of (0.15, 0.25) at operational voltages of 5–11 V (Figure 9). Notably, the device exhibited a very high luminance of 34 262 cd m^{-2} (Figure 10). To the best of our knowledge, this is the highest luminance reported for FIr6-based blue PhOLEDs.[40–51]
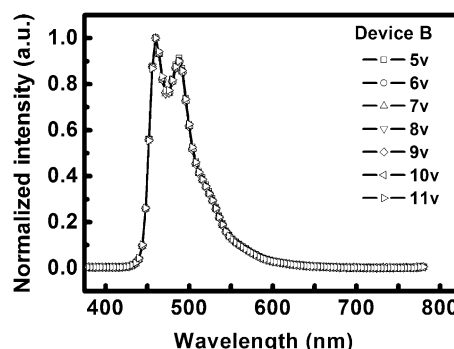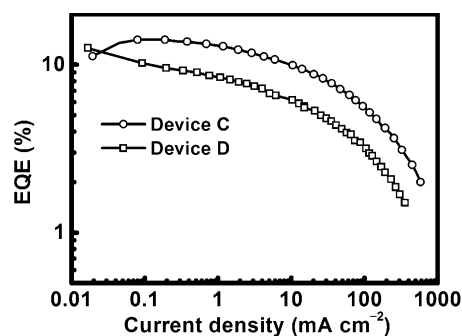

Figure 11. EQE of devices C and D.

esis, we measured the absolute photoluminescence quantum yields and transient decay spectra of the films with different concentrations of FIr6 doped into CzCN-Ad. The pure FIr6 film showed a PLQY of only 10%. However, a significant enhancement of PLQY was observed when CzCN-Ad was introduced to disperse the FIr6. High quantum efficiencies of 81 and 72% were achieved for concentrations of 6 and 10 wt%, respectively (Table 3). The lifetimes of films were all monoexponential

Table 3. PL lifetimes and quantum yields data for the films of TCTA/CzCN-Ad:x wt% FIr6 at room temperature.

Host	x [wt%]	$\tau^{[a]}$	$\chi^{2[b]}$	PLQY[c] [%]
TCTA	6	2.59	1.155	58
TCTA	10	2.44	1.063	51
TCTA	20	2.32	0.936	47
TCTA	40	2.14	1.121	43
TCTA	60	1.57	1.184	36
TCTA	80	0.98	0.974	22
CzCN-Ad	6	3.32	1.085	81
CzCN-Ad	10	3.25	1.019	72
CzCN-Ad	20	3.08	1.035	64
CzCN-Ad	40	2.76	1.141	62
CzCN-Ad	60	1.96	1.014	47
CzCN-Ad	80	1.15	1.220	28
FIr6		0.59	1.297	10

[a] Lifetimes of films. [b] Goodness of fit. [c] Photoluminescent quantum yields of films.

and in the range of microseconds. The pure FIr6 film showed a lifetime of only 0.59 μs, whereas relatively long lifetimes of 3.32 and 3.25 μs were observed for 6 and 10 wt% FIr6 films, respectively. These results confirmed that CzCN-Ad could effectively suppress T_1–T_1 annihilation and prevent reverse energy transfer. For comparison, films of TCTA doped with FIr6 were also fabricated. At the same doping concentration, all of the CzCN-Ad based films exhibited higher PLQYs and longer lifetimes than TCTA films. This implied that CzCN-Ad could suppress T_1–T_1 annihilation and reverse energy transfer more effectively than TCTA. The CzCN-Ad based films exhibited high PL efficiencies, which may account for the better EL performance of CzCN-Ad hosted devices over the TCTA hosted devices.

Conclusion

We have developed an adamantane-based host material. The rigid nonconjugated adamantane skeleton introduced an "sp³" configuration between electron-donating carbazole and electron-accepting benzonitrile moieties, and thus effectively broke the intramolecular charge transfer. This design endowed CzCN-Ad with a high triplet energy of 3.03 eV. Owing to the adamantane skeleton, CzCN-Ad showed a high T_g of 89 °C despite a low molecular weight of 478, which was favorable for evaporation. FIrpic-based sky-blue PhOLEDs hosted by CzCN-Ad exhibited a maximum current efficiency of 57.0 cd A^{-1}, a maximum power efficiency of 45.9 lm W^{-1}, and a maximum EQE of 24.1%. The FIr6-based PhOLED showed a high EQE of 14.2% and extremely high luminescence of 34 262 cd m^{-2}. This

excellent device performance demonstrated the great potential of adamantane-based compounds as host material for phosphorescent OLEDs.

Experimental Section

General information

^{1}H NMR and ^{13}C NMR spectra were measured on a Varian Unity 300 MHz spectrometer by using CDCl$_3$ as solvent and TMS as internal reference. Elemental analysis (C, H, N) was performed on a Vario EL-III microanalyzer. EI-MS spectra were recorded on a VJ-ZAB-3F-Mass spectrometer. DSC was performed on a NETZSCH DSC 200 PC unit at a heating rate of 10 °C min^{-1} from 20 to 300 °C under argon. T_g was determined from the second heating scan. TGA was performed with a NETZSCH STA 449C instrument and the thermal stability of the samples under nitrogen atmosphere was determined by measuring their weight loss at a heating rate of 10 °C min^{-1} from 25 to 600 °C. UV/Vis absorption spectrum was recorded on a Shimadzu UV-2550 spectrophotometer. PL spectra were recorded on a Hitachi F-4500 fluorescence spectrophotometer. The PL lifetimes and quantum yields were measured with a single-photon-counting spectrometer from Edinburgh Instruments (FLS920) with a picosecond pulsed UV-LED (EPLED330) as excitation source. The data were analyzed by iterative convolution of the luminescence decay profile with the instrument response function by using the software package provided by Edinburgh Instruments. CV measurements were carried out on a computer-controlled EG&G Potentiostat/Galvanostat model 283 with a solution of tetrabutylammonium hexafluorophosphate (0.1 M) as supporting electrolyte in freshly distilled CH$_2$Cl$_2$, and a conventional three-electrode cell with a Pt working electrode of 2 mm diameter, a platinum-wire counter electrode, and a Ag/AgCl reference electrode with ferrocenium/ferrocene (Fc$^+$/Fc) as internal standard was employed. All calculations (geometrical configurations and electronic properties) of CzCN-Ad were carried out with the Gaussian 09 program suite.[52]

Device fabrication and measurement

The hole-injection material MoO$_3$, hole-transporting materials 1,4-bis[(1-naphthylphenyl)amino]biphenyl (NPB) and 1,1-bis[4-[N,N-di(p-tolyl)-amino]phenyl]cyclohexane (TAPC), electron/exciton-blocking material 4,4′,4′′-tris(N-carbazolyl)triphenylamine (TCTA), and electron-transporting material 1,3,5-tris(m-pyrid-3-yl-phenyl)-benzene (TmPyPB) were commercially available (Luminescence Technology Corp.). Commercial indium tin oxide (ITO, 170 nm)-coated glass with sheet resistance of 10 Ω per square was used as the starting substrate. Before device fabrication, the ITO glass substrates were precleaned carefully and treated with oxygen plasma for 2 min. Then the sample was transferred to the deposition system. MoO$_3$ (10 nm) was first deposited on the ITO substrate, followed by NPB (100 nm) or TAPC (60 nm), TCTA (5 nm), emissive layer, and TmPyPB (35 nm). Finally, a cathode composed of lithium fluoride (1 nm) and aluminum (100 nm) was sequentially deposited onto the substrate under a vacuum of 10^{-6} Torr. Current density–voltage–luminance characteristics of the devices were measured by using a Keithley 2400 source meter and a Keithley 2000 source multimeter equipped with a calibrated silicon photodiode. The EL spectra were measured on a JY SPEX CCD3000 spectrometer. The EQEs were calculated according to previously reported methods.[53] All measurements were carried out at room temperature under ambient conditions.

Materials

1,3-Bis(4-iodophenyl)adamantane (**1**) was prepared according to previously reported procedures.[54] The solvents were dried by standard procedures. All other reagents were used as received from commercial sources unless otherwise stated.

Synthesis of 9-{4-[3-(4-iodophenyl)adamantan-1-yl]phenyl}-9H-carbazole (2): A mixture of **1** (1.1 g, 3.5 mmol), carbazole (0.58 g, 3.5 mmol), Cu_2O (1.2 g, 8.7 mmol), and dimethylacetamide (7.0 mL) was heated to reflux under argon for 24 h. After cooling, the mixture was extracted with CH_2Cl_2, washed with water, and the organic layer was dried over anhydrous Na_2SO_4. After removal of the solvent, the residue was purified by column chromatography on silica gel with CH_2Cl_2/petroleum (1/5 v/v) as the eluent to give a white powder. Yield: 50%. ^1H NMR (300 MHz, $CDCl_3$): $\delta = 8.15$ (d, $J = 6.9$ Hz, 2H), 7.67–7.59 (m, 4H), 7.53–7.42 (m, 6H), 7.32–7.26 (m, 2H), 7.19 (d, $J = 7.5$ Hz, 2H), 2.39 (s, 2H), 2.09–1.97 (m, 10H), 1.84 (s, 2H); ^{13}C NMR ($CDCl_3$, 75 MHz): $\delta = 29.48$, 35.74, 37.29, 37.36, 42.08, 42.20, 48.93, 91.13, 109.91, 119.82, 120.03, 123.31, 125.89, 126.37, 126.78, 127.27, 135.28, 137.30, 141.01, 149.65, 150.23; MS (EI): m/z 579.2; elemental analysis (%) calcd for $C_{34}H_{30}IN$: C 70.47, H 5.22, N 2.42; found: C 70.68, H 5.38, N 2.69.

Synthesis of 4-{3-[4-(9H-carbazol-9-yl)phenyl]adamantan-1-yl}-benzonitrile (CzCN-Ad): A mixture of **2** (1.2 g, 2.0 mmol), CuCN (0.29 g, 3.0 mmol), and DMF (3.0 mL) was heated to reflux for 4 h. After cooling, $FeCl_3$ (1.0 g) and hydrochloric acid (2.0 M, 1.8 mL) were added and the mixture heated at 70 °C for 0.5 h. After cooling, the mixture was extracted with CH_2Cl_2, washed with water, and the organic layer was dried over anhydrous Na_2SO_4. After removal of the solvent, the residue was purified by column chromatography on silica gel with CH_2Cl_2/petroleum (1/5 v/v) as eluent to give a white powder. Yield: 66%. ^1H NMR (300 MHz, $CDCl_3$): $\delta = 8.14$ (d, $J = 7.5$ Hz, 2H), 7.64–7.52 (m, 8H), 7.42–7.37 (m, 4H), 7.33–7.27 (m, 2H), 2.39 (s, 2H), 2.09–1.97 (m, 10H), 1.84 (s, 2H); ^{13}C NMR ($CDCl_3$, 75 MHz): $\delta = 29.57$, 35.83, 37.50, 38.19, 42.06, 42.26, 48.92, 109.84, 110.08, 119.41, 120.07, 120.54, 123.52, 126.12, 126.15, 126.56, 127.03, 132.38, 135.60, 141.17, 149.55, 156.02; MS (EI) m/z: 478.2; elemental analysis (%) calcd for $C_{35}H_{30}N_2$: C 87.83, H 6.32, N 5.85; found: C 88.09, H 6.13, N 6.08.

[1] Y. Tao, C. Yang, J. Qin, *Chem. Soc. Rev.* **2011**, *40*, 2943.
[2] M. A. Baldo, D. F. O'Brien, Y. You, A. Shoustikov, S. Sibley, M. E. Thompson, S. R. Forrest, *Nature* **1998**, *395*, 154.
[3] Y. Ma, H. Zhang, J. Shen, C. Che, *Synth. Met.* **1998**, *94*, 245.
[4] S.-J. Su, C. Cai, J. Kido, *J. Mater. Chem.* **2012**, *22*, 3447.
[5] C.-J. Zheng, J. Ye, M.-F. Lo, M.-K. Fung, X.-M. Ou, X.-H. Zhang, *Chem. Mater.* **2012**, *24*, 643.
[6] H. Sasabe, N. Toyota, H. Nakanishi, T. Ishizaka, Y.-J. Pu, J. Kido, *Adv. Mater.* **2012**, *24*, 3212.
[7] S.-J. Su, C. Cai, J. Kido, *Chem. Mater.* **2011**, *23*, 274.
[8] H.-H. Chou, C.-H. Cheng, *Adv. Mater.* **2010**, *22*, 2468.
[9] H.-H. Chou, H.-H. Shih, C.-H. Cheng, *J. Mater. Chem.* **2010**, *20*, 798.
[10] W. Li, J. Qiao, L. Duan, L. Wang, Y. Qiu, *Tetrahedron* **2007**, *63*, 10161.
[11] J. He, H. Liu, Y. Dai, X. Ou, J. Wang, S. Tao, X. Zhang, P. Wang, D. Ma, *J. Phys. Chem. C* **2009**, *113*, 6761.
[12] X. Ren, J. Li, R. J. Holmes, P. I. Djurovich, S. R. Forrest, M. E. Thompson, *Chem. Mater.* **2004**, *16*, 4743.
[13] S. Gong, N. Sun, J. Luo, C. Zhong, D. Ma, C. Yang, *Adv. Funct. Mater.* **2014**, *24*, 5710.
[14] H. Fukagawa, K. Watanabe, T. Tsuzuki, S. Tokito, *Appl. Phys. Lett.* **2008**, *93*, 133312.
[15] H. Fukagawa, N. Yokoyama, S. Irisa, S. Tokito, *Adv. Mater.* **2010**, *22*, 4775.
[16] H. Fukagawa, S. Irisa, H. Hanashima, T. Shimizu, S. Tokito, *Org. Electron.* **2011**, *12*, 1638.
[17] K.-R. Wee, Y.-J. Cho, S. Jeong, S. Kwon, J.-D. Lee, I.-H. Suh, S. O. Kang, *J. Am. Chem. Soc.* **2012**, *134*, 17982.
[18] S. Gong, Y. Chen, J. Luo, C. Yang, C. Zhong, J. Qin, D. Ma, *Adv. Funct. Mater.* **2011**, *21*, 1168.
[19] M.-H. Tsai, T.-H. Ke, H.-W. Lin, C.-C. Wu, S.-F. Chiu, F.-C. Fang, Y.-L. Liao, K.-T. Wong, Y.-H. Chen, C.-I. Wu, *ACS Appl. Mater. Interfaces* **2009**, *1*, 567.
[20] C. Fan, F. Zhao, P. Gan, S. Yang, T. Liu, C. Zhong, D. Ma, J. Qin, C. Yang, *Chem. Eur. J.* **2012**, *18*, 5510.
[21] H. Liu, Q. Bai, L. Yao, D. Hu, X. Tang, F. Shen, H. Zhang, Y. Gao, P. Lu, B. Yang, Y. Ma, *Adv. Funct. Mater.* **2014**, *24*, 5881.
[22] S. Gong, Q. Fu, W. Zeng, C. Zhong, C. Yang, D. Ma, J. Qin, *Chem. Mater.* **2012**, *24*, 3120.
[23] G. Zotti, G. Schiavon, S. Zecchin, J.-F. Morin, M. Leclerc, *Macromolecules* **2002**, *35*, 2122.
[24] Y. Tao, S. Gong, Q. Wang, C. Zhong, C. Yang, J. Qin, D. Ma, *Phys. Chem. Chem. Phys.* **2010**, *12*, 2438.
[25] J. Kalinowski, M. Cocchi, D. Virgili, V. Fattori, J. A. G. Williams, *Adv. Mater.* **2007**, *19*, 4000.
[26] K. S. Yook, J. Y. Lee, *Adv. Mater.* **2012**, *24*, 3169.
[27] M. Kim, J. Y. Lee, *ACS Appl. Mater. Interfaces* **2014**, *6*, 14874.
[28] C. Han, Z. Zhang, H. Xu, G. Xie, J. Li, Y. Zhao, Z. Deng, S. Liu, P. Yan, *Chem. Eur. J.* **2013**, *19*, 141.
[29] D. Yu, F. Zhao, C. Han, H. Xu, J. Li, Z. Zhang, Z. Deng, D. Ma, P. Yan, *Adv. Mater.* **2012**, *24*, 509.
[30] L. Xiao, Z. Chen, B. Qu, J. Luo, S. Kong, Q. Gong, J. Kido, *Adv. Mater.* **2011**, *23*, 926.
[31] A. Chaskar, H.-F. Chen, K.-T. Wong, *Adv. Mater.* **2011**, *23*, 3876.
[32] C. W. Lee, J. Y. Lee, *Adv. Mater.* **2013**, *25*, 596.
[33] C. W. Lee, J. Y. Lee, *Adv. Mater.* **2013**, *25*, 5450.
[34] D. Sun, X. Zhou, H. Li, X. Sun, Y. Zheng, Z. Ren, D. Ma, M. Bryce, S. Yan, *J. Mater. Chem. C* **2014**, *2*, 8277.
[35] M. Kim, J. Y. Lee, *Adv. Funct. Mater.* **2014**, *24*, 4164.
[36] H. Shin, S. Lee, K. H. Kim, C. K. Moon, S. J. Yoo, J. H. Lee, J. J. Kim, *Adv. Mater.* **2014**, *26*, 4730.
[37] X. Yuan, J. Liang, Y. He, Q. Li, C. Zhong, Z. Jiang, L. Liao, *J. Mater. Chem. C* **2014**, *2*, 6387.
[38] L. Cui, Y. Liu, Q. Li, Z. Jiang, L. Liao, *Org. Electron.* **2014**, *15*, 1368.
[39] S. Gong, Y. Chen, C. Yang, C. Zhong, J. Qin, D. Ma, *Adv. Mater.* **2010**, *22*, 5370.
[40] S. Ye, Y. Liu, C.-A. Di, H. Xi, W. Wu, Y. Wen, K. Lu, C. Du, Y. Liu, G. Yu, *Chem. Mater.* **2009**, *21*, 1333.
[41] S.-H. Eom, Y. Zheng, N. Chopra, J. Lee, F. So, J. Xue, *Appl. Phys. Lett.* **2008**, *93*, 133309.
[42] S. Gong, Q. Fu, Q. Wang, C. Yang, C. Zhong, J. Qin, D. Ma, *Adv. Mater.* **2011**, *23*, 4956.
[43] S.-H. Eom, Y. Zheng, E. Wrzesniewski, J. Lee, N. Chopra, F. So, J. Xue, *Org. Electron.* **2009**, *10*, 686.
[44] J. Lee, J.-I. Lee, J.-W. Lee, H. Y. Chu, *Org. Electron.* **2010**, *11*, 1159.
[45] Y.-H. Niu, M. S. Liu, J.-W. Ka, A. K. Y. Jen, *Appl. Phys. Lett.* **2006**, *88*, 093505.
[46] M. Liu, Y.-H. Niu, J.-W. Ka, H.-L. Yip, F. Huang, J. Luo, T.-D. Kim, A. K. Y. Jen, *Macromolecules* **2008**, *41*, 9570.
[47] Y. Zheng, S.-H. Eom, N. Chopra, J. Lee, F. So, J. Xue, *Appl. Phys. Lett.* **2008**, *92*, 223301.
[48] J. Lee, J.-I. Lee, J. Y. Lee, H. Y. Chu, *Appl. Phys. Lett.* **2009**, *95*, 253304.
[49] S. Gong, Y. Chen, X. Zhang, P. Cai, C. Zhong, D. Ma, J. Qin, C. Yang, *J. Mater. Chem.* **2011**, *21*, 11197.

[50] C.-A. Wu, H.-H. Chou, C.-H. Shih, F.-I. Wu, C.-H. Cheng, H.-L. Huang, T.-C. Chao, M.-R. Tseng, *J. Mater. Chem.* **2012**, *22*, 17792.

[51] R. J. Holmes, B. W. D'Andrade, S. R. Forrest, X. Ren, J. Li, M. E. Thompson, *Appl. Phys. Lett.* **2003**, *83*, 3818.

[52] Gaussian 09, Revision 5.08, M. J. Frisch, G. W. Trucks, H. B. Schlegel, G. E. Scuseria, M. A. Robb, J. R. Cheeseman, G. Scalmani, V. Barone, B. Mennucci, G. A. Petersson, H. Nakatsuji, M. Caricato, X. Li, H. P. Hratchian, A. F. Izmaylov, J. Bloino, G. Zheng, J. L. Sonnenberg, M. Hada, M. Ehara, K. Toyota, R. Fukuda, J. Hasegawa, M. Ishida, T. Nakajima, Y. Honda, O. Kitao, H. Nakai, T. Vreven, J. A. Montgomery, Jr., J. E. Peralta, F. Ogliaro, M. Bearpark, J. J. Heyd, E. Brothers, K. N. Kudin, V. N. Staroverov, R. Kobayashi, J. Normand, K. Raghavachari, A. Rendell, J. C. Burant, S. S. Iyengar, J. Tomasi, M. Cossi, N. Rega, J. M. Millam, M. Klene, J. E. Knox, J. B. Cross, V. Bakken, C. Adamo, J. Jaramillo, R. Gomperts, R. E. Stratmann, O. Yazyev, A. J. Austin, R. Cammi, C. Pomelli, J. W. Ochterski, R. L. Martin, K. Morokuma, V. G. Zakrzewski, G. A. Voth, P. Salvador, J. J. Dannenberg, S. Dapprich, A. D. Daniels, Ö. Farkas, J. B. Foresman, J. V. Ortiz, J. Cioslowski, D. J. Fox, Gaussian, Inc. Wallingford CT, **2009**.

[53] S. R. Forrest, D. D. C. Bradley, M. E. Thompson, *Adv. Mater.* **2003**, *15*, 1043.

[54] S. Zheng, J. Shi, R. Mateu, *Chem. Mater.* **2000**, *12*, 1814.